BEHAVIOUR OF CRACKED CYLINDERS UNDER COMBINED THERMAL AND MECHANICAL LOADING

S. IGNACCOLO*, B. DRUBAY ✸, B. MICHEL✧, P. GILLES✣

In the field of non linear fracture mechanics a lot of work has been achieved for structures submitted to mechanical loadings. But for thermal loadings, and particularly for thermal shocks, only few contributions are available. We propose, here, to present the main results of a complete set of finite element computations, conducted by CEA, EDF and FRAMATOME, on cracked cylinders submitted to combined mechanical and thermal loads. The interaction between these two types of loads is analysed in the cases of austenitic and ferritic structures.

Moreover, these results are compared to the predictions obtained by simplified engineering methods (R6 procedure and two French approaches). Their domain of validity is also discussed.

INTRODUCTION

Nuclear pressure vessels or pipings can be submitted in their life to severe mechanical and thermal loadings. In this type of structure we need engineering methods easy to apply but as accurate as possible to assess the flaws. In this paper we study the basic problem of a cylinder with an inner circumferential surface crack under combined pressure, tension and thermal gradient in the thickness. The scope here is to improve simplified rules in non-linear fracture mechanics through the understanding of the behaviour of these cylinders. After the presentation of the non-linear computational program and the simplified methods tested, we discuss the results and give some recommandations on their application.

VALIDATION PROGRAM

A set of configurations representative of the nuclear industry components have been achieved and constitute the reference data base to assess the simplified rules. The basic model is an axisymmetrically cracked cylinder (figure 1) submitted, separately or simultaneously, to pressure : σ_{Pi}, tension: σ_{zz}, and thermal gradient in the thickness : ΔT.

* EDF/ 12-14 Avenue Dutrievoz 69628 Villeurbanne
✸ CEA/DMT/SEMT/RDMS 91191 Gif sur Yvette
✧ CEA/DER/SERA/LDCS 13108 St Paul lez Durance
✣ FRAMATOME/Tour FRA 92084 Paris la Défense

The non-dimensional parameters are presented in table 1. Since the effect of pressure is studied, the load combination factors are given in table 2.

t (mm)	60				40			
R_m/t	5		10		5		10	
a/t	1/8	1/4	1/8	1/4	1/8	1/4	1/8	1/4

Table 1: non-dimensional parameters studied

The thermal gradient superposed to this primary loads is such as : $0 < \frac{E\alpha\Delta T}{2\sigma_y} < 3$

		$\sigma_{\theta\theta}/\sigma_y$			
		0	0,4	0,8	1
σ_{zz}/σ_y	0	C9			
	0,5				C10
	0,8	C1	C3	C5	C7
	1		C11	C13	
	1,2	C2	C4	C6	C8
	1,4		C12	C14	

Table 2: Cases of primary load combinations studied

Two types of material have be taken into account : ferritic and austenitic steel, which tensile stress-strain curves are presented in figure 2. The particularity of the first one is to present a pronounced flat plateau at the yield point.

More than thirty two-dimensional elastic-plastic (small transformations assumption) configurations have been computed with essentially two finite element codes : CASTEM 2000 for C.E.A. and ASTER for EDF.

The fracture parameter J integral is obtained using G-θ method [1],[2] validated only under the Deformation Plasticity Theory assumptions [3]. We consider that this is nearly true in our cases since J is constantly increasing.

SIMPLIFIED METHODS

Mechanical loading

All the following methods to estimate J-integral (R6, J_{SA16}, J_{EDF}) are based, for the mechanical part, on the plastic correction of the K_I factor using the reference stress technique as established by Ainsworth in R6 procedure [4]. This reference stress (σ_{ref}) is deduced from the limit analysis of the structure containing the defect and is given as a function of the membrane and bending elastic stresses in the flawed structure.The general scheme can be summerized under plane strain assumption by :

$$J_e = \frac{(1-\nu^2)\times K_I^{\,2}}{E} \quad \text{and} \quad J = \frac{J_e}{K_r^{\,2}} \qquad K_r = \frac{1}{\sqrt{\frac{L_r^{\,3}\times\sigma_y}{2E\times\varepsilon_{ref}} + \frac{E\times\varepsilon_{ref}}{L_r\times\sigma_y}}} \qquad \text{and} L_r = \frac{\sigma_{ref}}{\sigma_y}$$

where: K_I, the stress intensity factor may be obtained by finite elements or influence function method,

σ_y is the engineering yield strength

σ_{ref} is the reference stress in the cracked section

ε_{ref} is the reference strain corresponding to the σ_{ref} on the uniaxial tensile stress strain curve of the material.

The reference stress is deduced from one of the three following equivalent stress models :

1D beam: $\sigma_{1D} = \frac{\sigma_{1b}}{3} + \sqrt{\sigma^2{}_{1m} + \left(\frac{\sigma_{1b}}{3}\right)^2}$

2D panel [5]: $\sigma_{2D} = \sqrt{0.75 \times \sigma_{2m}^2 + \left[\frac{\sigma_{1b}}{3} + \sqrt{\left(\sigma_{1m} - \frac{\sigma_{2m}}{2}\right)^2 + \left(\frac{\sigma_{1b}}{3}\right)^2}\right]^2}$

3D panel [3]:

$$\sigma_{3D} = \sqrt{\begin{bmatrix}\sigma_{1m}^2 + \sigma_{2m}^2 \\ -.\sigma_{1m} \times \sigma_{2m}\end{bmatrix} + \left(\frac{2}{3\sqrt{3}}\right) \times \begin{vmatrix}\sigma_{1m} \times \sigma_{1b} + \sigma_{2m} \times \sigma_{2b} \\ -0.5(\sigma_{1m} \times \sigma_{2b} + \sigma_{2m} \times \sigma_{1b})\end{vmatrix} + \left(\frac{2}{3}\right)^2 \begin{bmatrix}\sigma_{1b}^2 + \sigma_{2b}^2 \\ -.\sigma_{1b} \times \sigma_{2b}\end{bmatrix}}$$

σ_{1m} and σ_{2m} are respectively axial and circumferential membrane stresses

σ_{1b} and σ_{2b} are respectively axial and circumferential bending stresses

This last formula has been used for the reference stress, in the following applications, to take into account of circumferential membrane and bending stresses.

Combined mechanical and thermal loading

In case of combined loading , we need first of all a classification in primary (P) and secondary (Q) stresses (for instance, thermal stresses are considered secondary) on which depends the value of the reference load . We need also a way to take into account the influence of both types of stresses. On this last point the three methods differ.

R6 procedure

For R6 procedure, K_r parameter is modified by a ρ factor which depends on L_r parameter and on the proportion of secondary and primary stresses (figure 3)[6] :

$$J_{R6} = \frac{J_e}{(K_r - \rho)^2}$$

A16 procedure

The J_{SA16} method introduced in the document A16 [7] proposes to take into account the difference between the nominal stresses far from the cracked section (signo) and in the ligament (sigdef). The J_e value is corrected by 2 factors : k_{1A16} related to signo$(P+Q)_{eq}$ and signo$(P)_{eq}$ (figure 4); k_{2A16} depending on sigdef$(P+Q)_{eq}$ and sigdef$(P)_{eq}$ (figure 5).

$$k_{1A16} = \left(\frac{\sigma_{nor}}{\text{signo}(P+Q)_{eq}} \right)^2 \text{ and } k_{2A16} = \left(\Psi_{A16} + \frac{E \times \varepsilon_{ref}}{\sigma_{ref}} \right)$$

where $\Psi_{A16} = \frac{0.5\sigma_{ref}}{\sigma_{ref}^2 + \sigma_y^2}$ $\quad J_{SA16} = J_e \times k_{1A16} \times k_{2A16}$

Moreover, when we have secondary stresses : $\sigma_{nor} \neq \text{signo}(P)_{eq}$ and Neuber extrapolation $\sigma_{ref} \neq \text{sigdef}(P)_{eq}$.

EDF procedure

As far as primary stresses are concerned, J_{EDF} method involved in the French RSE-M [8] is the same as R6 one. For the thermal stresses J_e^{th} is multiplied by the $(k_{th})^2$ factor fitted on the results of an important set of finite element computations [9] covering the domain : $0.07 \leq \frac{a}{t} \leq 0.3$ and $6 \leq \frac{R_i}{t} \leq 17$

$$k_{th} = Min\left[1; 0.5 + 0.5\exp(\beta - 0.4 L_{th})\right] \text{ with } L_{th} = \frac{EaDT_1}{2(1-n)} \times \frac{\left(1-5\left(\frac{a}{t}\right)^2\right)}{s_y} < 3$$

This last formula depends on the material : for austenitic steels under linear temperature gradients $\beta = 0.32$. For ferritic steel we have $\beta = 0.44$.

Finally, mechanical and thermal terms are combined as follow :

$$J_{EDF} = \left(\sqrt{\frac{J_e^{meca}}{K_r^2}} + k_{th}\sqrt{J_e^{th}} \right)^2$$

These three procedures have been tested and compared to the finite element results.

APPLICATIONS AND COMPARISON OF THE DIFFERENT APPROACHES

Since it is impossible to give all the computational results, we have selected for the comparisons two geometries and two different materials defined as follow :

austenitic steel : $R_m = 300$ mm ; $R_m/t = 5$; $a/t = 1/4$;
$E = 176\,500$ MPa; $\sigma_y = 133$ MPa ; $\nu = 0.3$; $\alpha = 17.7.10^{-6}$ °C^{-1} ; $\lambda = 18.6$ W(m.°C)$^{-1}$

ferritic steel : $R_m = 400$ mm ; $R_m/t = 10$; $a/t = 1/4$;
$E = 191\,837$ MPa ; $\sigma_y = 188$ MPa ; $\nu = 0.3$; $\alpha = 12.9.10^{-6}$ °C^{-1} ; $\lambda = 45.8$ W(m.°C)$^{-1}$

Pure thermal loading : The gradient in the thickness, ΔT, is applied progressively from 0 to 180°C. The finite element results (figure 6) show the elastic J_e and elastic-plastic J solution in terms of J-integral. When the yield stress is exceeded the plastic solution becomes lower than the elastic J_e. This is due to the relaxation of the secondary stresses. The comparison with the simplified methods is given in figure 7. J_{EDF} curve is the closest from elastic-plastic solution. J_S method give results reasonably conservative.

Plasticity effects becomes rapidly (σ_{zz}>0.7xσ_y) very strong (J/J_e=10). When we look at the simplified methods results we conclude that no method predicts the right value (figure 8). This is true particularly when the part of the pressure becomes non-negligible in the mechanical loading. That means that another stress parameter is required to complete the reference stress definition to include the effect of pressure on the limit load [10].

Combined mechanical and thermal loading : When the last mechanical loading is combined with the first thermal one, the J_e remains lower than J because the influence of the mechanical load is stronger; but the ratio J/J_e decreases below the value of 2. This is reproduced quite accurately by the J_S and J_{EDF} methods (figure 9) if we start from the good mechanical estimation. R6 results are not shown here because they are too conservative(J_{R6}/J =4).

To complete this set of results we give the comparison of the results of the different methods for a ferritic steel. The same combined loading as above has been applied to a cracked cylinder (R_m/t = 10).

When the yield point is reached the plasticity correction climbs up very rapidly so that estimated J becomes higher than J-integral at the end of the application of the mechanical loading (figure 10). J_{EDF} curve on figure 11 diverges from the finite element curve at high thermal loading level because the key curve used to represent the ferritic behaviour does not match well the stress-strain curve at high stress level.

CONCLUSION

When simplified methods, like R6-option 2, are applied on cylinders submitted to combined mechanical loading, it is important to take into account in the reference stress expression, not only the opening stresses but also hoop stresses for high load level.

For ferritic steels,that exhibit a yield plateau, the approach must be improved particularly in the vicinity of the yield point.

R6-option 2 is too conservative in the case of thermal loading specially when it is combined with a primary load. The two other methods (J_{SA16} and J_{EDF}) takes better into account the secondary stress relaxation while remaining conservative.

The computational program will be completed by thermal shocks , 3D computations of semi-elliptical flaws under bending and thermal stresses, and on other crack geometries submitted to primary and secondary loads. The improved simplified methods will also be applied and assessed for these more realistic configurations.

REFERENCES

[1] Destuynder,Ph.,Djaoua,M. "Sur une interprétation mathématique de l'intégrale de Rice en théorie de la rupture fragile", Mathematical Methods and Applied Sciences, Vol.3, pp.70-87, 1981

[2] De Lorenzi,H.G. "3-D Elastic Plastic fracture mechanics with ADINA", Computers and Structures, Vol. 13, pp.613-621, 1981.

[3] Illyushin,A.A "Plasticité-déformations élastoplastiques", Eyrolles, 1956.

[4] Ainsworth,R.A. "The assessment of defect in structures of strain hardening material", Engineering Fracture Mechanics, Vol. 19 , pp.633-642, 1984

[5] Miller,A.G. "Review of limit loads of structures containing defects", The international journal of pressure vessels and piping. Vol. 32 p.228, 1988

[6] Milne,I., Ainsworth,R.A., Dowling,A.R. ,Stewart,A.T. "Background to and validation of CEGB Report R/H/R6 - Revision 3" The international journal of pressure vessels and piping. Vol. 32 p.105, 1988

[7] Drubay, B, Moulin, D, Faidy, C, Poette,C, Bhandari,S. "Defect assessment procedure: a French approach for fast breeder reactors" SMIRT 12-Vol.A-pp.139-144-Stuttgart-1993

[8] Barthelet,B , Le Delliou,P. , Heliot,J. , Faidy,C. , Drubay,B. "RSE-M code progress in the field of examination evaluation and flaw acceptance criteria" SMIRT 13-Porto Allegre- 1995

[9] Barthelet,B , Coustillas,F. , Pollez,P. "Simplified evaluation of J integral in cylinders under thermal loading" SMIRT 13-Porto Allegre- 1995

[10] Desquines,J , Poette,C. , Lejeail,Y, Martelet,B. "Limit loads: influence of hoop pressure terms in the case of circumferentially cracked pipe under combined bending and pressure." SMIRT 13-Porto Allegre- 1995

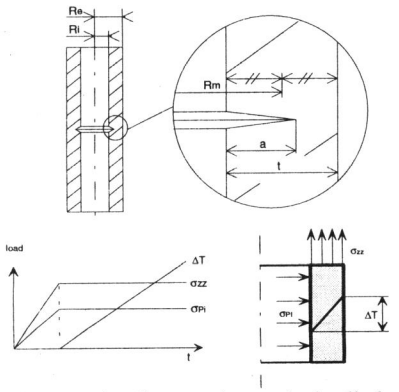

Figure 1 : loadings on the cracked cylinder

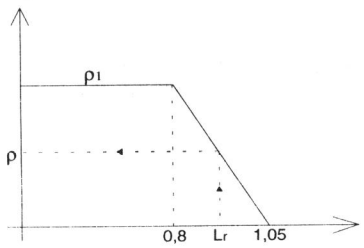

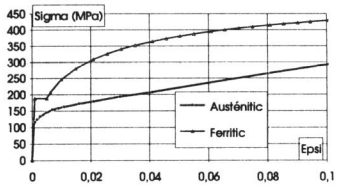

Figure 2 : Stress-strain curves for austenitic and ferritic steels

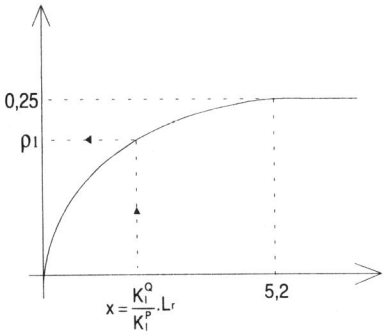

Figure 3 : secondary stress factor ρ

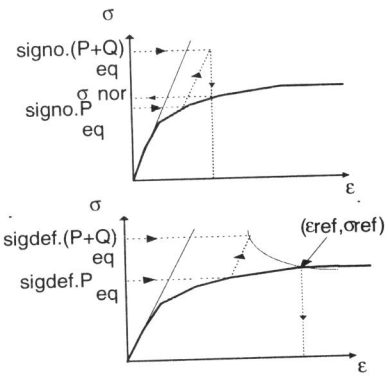

Figure 4 : k_{1A16} and Figure 5 : k_{2A16}

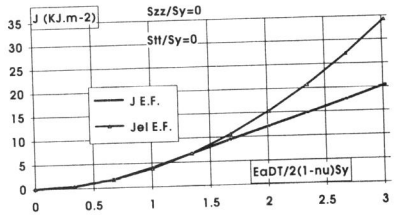

Figure 6 : Finite Element results for J and Je under thermal loading

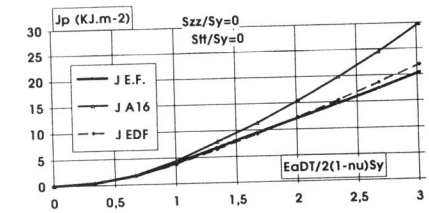

Figure 7 : Simplified method results for J under thermal loading

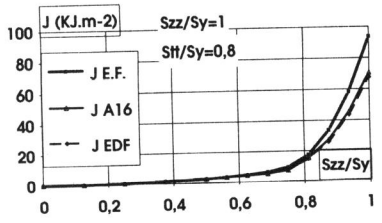

Figure 8 : Simplified method results for J under mechanical loading

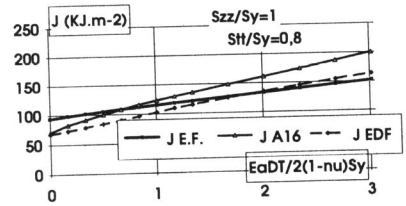

Figure 9 : Simplified method results for J under combined loading

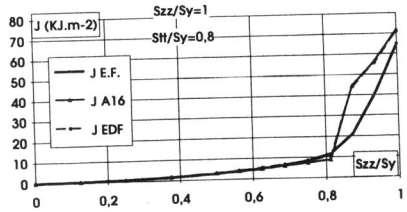

Figure 10 :Simplified method results for J under mechanical loading on ferritic steel

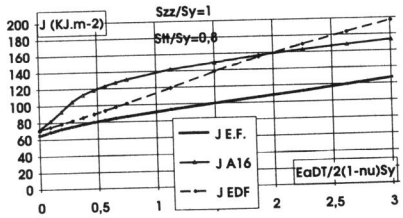

Figure 11 : Simplified method results for J under combined loading on ferritic steel